

# Oceanic Forces and their Impact on the Performance of Mobile Underwater Acoustic Sensor Networks

Amit Kumar Mandal<sup>\*†</sup>, Sudip Misra<sup>\*</sup>, Tamoghna Ojha<sup>\*</sup>, Mihir Kumar Dash<sup>†</sup>, and Mohammad S. Obaidat<sup>‡</sup>

<sup>\*</sup> School of Information Technology, Indian Institute of Technology, Kharagpur, 721302, India

Email: amiiit.mandal@gmail.com, {smisra, tojha}@sit.iitkgp.ernet.in

<sup>†</sup> Center for Oceans, Rivers, Atmosphere and Land Sciences, Indian Institute of Technology, Kharagpur, 721302, India

Email: mihir@coral.iitkgp.ernet.in

<sup>‡</sup> Department of Computer Science and Software Engineering, Monmouth University, West Long Branch, NJ 07764, USA

Email: obaidat@monmouth.edu

**Abstract**—This paper focuses on the performance analysis of Underwater Wireless Acoustic Sensor Networks (UWASNs) with passively mobile sensor nodes moving due to the influence of major oceanic forces. In an UWASN, passive node mobility is inevitable. Therefore, the performance analysis of UWASNs renders meaningful insights with the inclusion of a mobility model which represents realistic oceanic scenarios. In this regard, the existing works on performance analysis of UWASNs lack the consideration of major dominating forces, which offer impetus for a node's mobility. Additionally, the existing works are limited to only shallow depths and coastal areas. Therefore, in this paper, we have proposed a physical mobility model, named *Oceanic Forces Mobility Model (OFMM)*, by incorporating important realistic oceanic forces imparted on nodes. The proposed model considers the effects of node mobility in 3-D space of water. We also present an analysis on the impact of node mobility on the performance of UWASNs in terms of network dispersion and localization. Simulation results indicate performance degradation of UWASNs in the presence of oceanic forces — localization coverage decreases by 36.70%, localization error increases nearly by 21.14%, and average energy consumption increases by 3% approximately.

**Index Terms**—Oceanic forces, node mobility, acoustic signal, underwater wireless acoustic sensor network

## I. INTRODUCTION

UWASNs consist of acoustic communication enabled sensor nodes deployed in a particular oceanic underwater region of interest to perform collaborative monitoring task. The advent of UWASNs spurred a new direction of research on information transmission and retrieval in ocean-based applications [1], [2], [3], [4]. Few potential applications of UWASNs include real-time ocean environment monitoring [5], [6], pollution monitoring and control [5], intrusion detection and target tracking [7], [8], guided navigation, and disaster prevention [3], [9], [10], [11], [12]. However, UWASNs pose several fundamental challenges [1], [2], [3], [13], [14], [15], node mobility being one of them [16], [17], [18]. It is also an inherent aspect of UWASNs.

The existing literature on UWASNs consider various issues such as node localization [18], [19], target tracking [7], [8], jamming [20], [21], network architecture [17], routing [22]. Unfortunately, in terms of performance evaluation of UWASNs [23], [24], these works either did not consider the node mobility aspect or followed mobility model with limited scope. In

this regard, we can analyze the performance of the UWASNs in two ways — field test experiment or simulation. Field test experiments impose huge deployment and maintenance cost, while the simulations are effective in carrying out a study prior to the execution of field experiments. Therefore, we propose a node mobility model for UWASNs considering major oceanic forces. Consequently, we follow the simulation-based approach for performance evaluation to validate our theoretical study.

### A. Main Challenges in Building Mobile UWASNs

Being resource-constrained, a UWASN design demands improved efficiency in terms of energy, computation, and communication capabilities [16].

- Underwater nodes are resource-constrained. Also, they can not be recharged remotely. Over time, node's energy resource, i.e., battery, is drained out mainly due to communication and computation.
- Disruption of network collaboration (routing, data aggregation, localization) takes place due to node's mobility.
- As the quality of data transmission depends on the product,  $bandwidth \times delay$ , fluctuation in data transfer results due to change in delay of data transmission in between the nodes.

### B. Motivation

Oceanic environment is inherently dynamic in nature. Consequently, the deployed sensor nodes experience passive movement in such environment. Literature exist [25], [26], [27] on the dynamical aspects of UWASNs. In those works, the node's movement is limited to the 2-D horizontal plane only. Additionally, those models do not incorporate the major active oceanic forces. In those works, simulations are mainly carried out by considering the kinematic aspects of a network.

### C. Contribution

In this paper, we propose a node mobility model, named *Oceanic Forces Mobility Model (OFMM)*, considering the major forces acting on a node deployed in an UWASN. We discuss the relevant major oceanic forces, and present

a detailed analysis of their impact. The proposed mobility model represent node movement in the 3-D space of ocean. Consequently, this paper analyzes the performance of mobile UWASNs in terms of network dispersion and localization. Our main *contributions* in this work are listed below as:

- We present a thorough analysis of major oceanic forces exerting on an underwater sensor node.
- We propose a underwater sensor node mobility model which represents 3-dimensional movement of nodes.
- We numerically solve the motion of a node in vertical plane and on the basis of that we express the dynamical behavior of that node in that plane.

#### D. Paper Organization

The rest of the paper is organized as follows. Section II presents a brief survey of the related literature, and inferences the research gap. We discuss the relevant oceanic forces which impact the motion of deployed nodes in Section III. The proposed mobility model and its theoretical framework are presented in Section IV. Section V depicts the network architecture representation. We discuss the effects of node mobility on the performance of UWASNs in Section VI. The simulation-based results are presented and discussed in Section VII. Finally, in Section VIII, the paper concludes while citing few future research directions.

## II. RELATED WORKS

In the last decade, a number of research works were carried out on the mobility aspect of nodes in underwater sensor network. In [28], Caruso et al. proposed a physically inspired mobility model, named the *Meandering Current Mobility Model (MCM)*, which is a representative of underwater environments in coastal areas. The authors mainly studied the effect of their model on the range-based localization protocol. Additionally, they analyzed network connectivity, coverage, and deployment of network. However, according to this model, the nodes are subjected to move under the effect of a sub-surface current, which is known as meandering current. Therefore, in their model, node's mobility is confined to a particular plane, and henceforth, this model is not sufficient to describe the movement of underwater sensors in 3-D space.

Cui et al. [16] outlined the challenges in building a large-scale scalable mobile UWASN. Particularly, the authors adopted a top-down approach to explore the research challenges in mobile UWASN design. At each layer, they studied a set of new design intricacies. However, in their work, they did not consider any realistic oceanic forces which influence the movement of sensor nodes. Erol et al. [29] proposed a framework to establish localization and routing in mobile UWASNs. Localization and routing were done in two different contexts — where localization messages include localization-specific data and few extra fields were used to facilitate the routing decision. Furthermore, the authors considered mobile beacons for location servers as well as for the sinks. The proposed algorithm also uses position and velocity information of the sensors, which move under the effects of jet current

[29]. However, they did not consider movement of nodes in 3-D space under the realistic oceanic forces.

Luo et al. [30] studied a double mobility coverage problem. This work consists of two types of mobility — one is uncontrolled mobility or *U-mobility* by the sea flows, and another is the controlled mobility or *C-mobility* by the sensor nodes. The authors concluded that U-mobility disrupts the coverage of the sensor network, however, at the same time, sends the sensor nodes to the location that might improve coverage. The key target of this work was to minimize energy consumption of the sensor nodes while providing guaranteed coverage to the points of interest. Towards this direction, the authors leveraged U-mobility, and minimized the movement distance in C-mobility to balance the energy consumption of the nodes. However, in this work, the node's mobility is confined to a plane, and thus, it is unable to support 3-D movement of nodes.

Erol-Kantarci et al. [31] considered the nodes to float several meters below the surface and move with the force of current. In this work, the authors compared the performance of three localization techniques, namely — Dive and Rise Localization (DNRL), Proxy Localization (PL) and Large-Scale Localization (LSL). All of these techniques are distributed, range-based localization schemes and they are suitable for large-scale, three dimensional, mobile UWASNs. Ref. [31] introduced the concept of mobility of underwater sensor node, however, this work is silent about addressing the major oceanic forces causing the movement of these nodes. Yang et al. [32] proposed a mobility model for 3-D underwater acoustic sensor networks. Their model is based on the Lagrange motion of submerged nodes. However, in their model, 3-D movement of nodes is not reflected. They considered different independent layers and showed the layered movement of nodes. Kostin et al. [33] evaluated the performance of wireless mobile ad-hoc network with orientation dependency in inter-node communication. However, in this work, the authors did not consider active oceanic forces causing the movement of nodes.

The literature survey reveals that the existing mobility models are limited to only 2-dimensional UWASN scenarios. Also, the existing mobility models do not include major oceanic forces in their model. We propose a mobility model, *Oceanic Forces Mobility Model (OFMM)*, which includes major oceanic forces and clearly take into account the 3-D movement of nodes.

## III. MAJOR OCEANIC FORCES

Ocean is subjected to few governing factors [34] such as the following:

- The first and foremost factor is *Gravity*. The ocean water mass produces pressure. Gravity is responsible for producing *Gravitational force*. The *Pressure gradient force* is the result of varying weight of water in different regions of the ocean.
- The second factor is *Friction*. It arises when a body moves past another body in contact. The force due to friction is known as *Frictional force*.

- The other noteworthy factor is the *rotation of the Earth* on its own axis. This factor leads to two important forces as: *Centrifugal force* and *Coriolis force*.

As the forces stated above are the consequence of the dominating factors in the ocean, we denote them as major oceanic forces. These forces are discussed with their mathematical expression in detail below as:

- **Pressure Gradient Force (PGF):**

It arises due to non-uniform spatial distribution of pressure. It directs from a higher pressure region to a lower one. PGF tends to make movement of mass along its direction. PGF,  $F_p$ , can be mathematically expressed as:

$$F_p = -\frac{1}{\rho} \vec{\nabla} p \quad (1)$$

In Equation (1),  $\rho$  is the density of ocean water, and  $\vec{\nabla} p$  is pressure gradient term. If pressure gradient force was the only force acting in the ocean, there would have been only unidirectional movement of any object existing in the ocean from high pressure to low pressure region [34]. However, this is not so in real. Because, along with this force, simultaneously other forces also act on the body.

- **Coriolis Force (CF):**

Coriolis force is the most dominating pseudo-force influencing motion in a co-ordinate system fixed to the Earth [35]. This force arises due to the spinning motion of the Earth on its own vertical axis. This is also known as apparent deflection force which depends on the velocity ( $V$ ) with which a body moves, angular velocity ( $\omega$ ) of the Earth, and latitude,  $\phi$ . Coriolis force,  $F_c$ , can be mathematically expressed as:

$$\vec{F}_c = -2(\vec{\omega} \times \vec{V}) \quad (2)$$

In the northern hemisphere, CF acts in the clockwise direction, and in the southern hemisphere it acts in the counter-clockwise direction.

- **Force due to gravity:**

This force is exerted by the Earth on any celestial body. Gravitational force,  $F_g$ , due to unit mass can be expressed as:

$$\vec{F}_g = -\vec{g} \quad (3)$$

In Equation (3), negative sign in the right hand side has been put due to the fact that gravitational force is acting vertically downward, i.e., along negative Z direction. Change in gravity due to motion of the sun and the Moon, relative to Earth produces tides, tidal current, and the tidal mixing in the interior of the ocean [35].

- **Frictional force:**

This force arises due to relative motion between any two adjacent ocean water layers. It acts tangentially along the interface of the two layers. Mathematically, it can be expressed as:

$$\vec{F}_r = \nu \nabla^2 \vec{V} \quad (4)$$

In Equation (4),  $\nu$  is known as co-efficient of dynamic viscosity. For example wind stress is the friction arises due to wind blowing across the sea surface.

#### IV. PROPOSED MOBILITY MODEL

In this section, we propose a new mobility model which we call as the *Oceanic Forces Mobility Model (OFMM)*. To establish the proposed model, initially, we have taken the help of Navier Stoke's equation [34], which includes all the forces described in Section III. The Navier Stoke's equation is expressed as [34]:

$$\frac{dV}{dt} = -\frac{1}{\rho} \vec{\nabla} p - 2(\vec{\omega} \times \vec{V}) - \vec{g} + \nu \nabla^2 \vec{V} \quad (5)$$

Equation (5) can be expressed in three components form: X-, Y-, and Z-component. We made certain assumptions pertaining to the components form of Navier-Stoke's equation. Those *assumptions* are stated below:

- We neglected the effect of Coriolis force in the networking scenario, because this force has significant effect on a very large scale motion of a dynamical body. However, in our scenario, the nodes move in a very small-scale region. Therefore, the exclusion of its effect does not make any significant impact in our calculation. So, we have omitted this term in the force equation.
- We assumed pressure to vary along vertical direction with increasing depth. In a particular plane, it is constant throughout. On the basis of this assumption, we mathematically express the linear variation of pressure as:

$$\frac{\partial p}{\partial x} = \frac{\partial p}{\partial y} = 0 \quad (6)$$

$$\frac{\partial p}{\partial z} > 0 \quad (7)$$

Considering the assumptions made in the Section III, Equation (5) is represented in components form as:

$$X - Component : \frac{dV_x}{dt} = \nu \frac{\partial^2 V_x}{\partial x^2} \quad (8)$$

$$Y - Component : \frac{dV_y}{dt} = \nu \frac{\partial^2 V_y}{\partial y^2} \quad (9)$$

$$Z - Component : \frac{dV_z}{dt} = -\frac{1}{\rho} \frac{\partial p}{\partial x} - g + \nu \frac{\partial^2 V_z}{\partial z^2} \quad (10)$$

In the above equations,  $V_x$ ,  $V_y$ , and  $V_z$  are respectively the X-, Y-, and Z-components of velocities.

##### A. Solution Approach of the Component Equations

1) *X-component Equation:* Rearranging Equation (8), we have:

$$\frac{d^2 V_x}{dx^2} - \frac{1}{\nu} \frac{dV_x}{dt} = 0 \quad (11)$$

Let,  $\phi(V_x) = \frac{dV_x}{dx}$ . Therefore,  $\frac{d^2 V_x}{dx^2} = \frac{d}{dx}(\phi) = \phi \frac{d\phi}{dV_x}$ . Substituting these values in Equation (11), we have the finalized expression for X-component as:

$$\phi \frac{d\phi}{dV_x} - \frac{1}{\nu} \phi V_x = 0 \quad (12)$$

Dividing both sides by  $\phi$  and rearranging Equation(12), we can write it as:

$$\frac{d\phi}{dV_x} = \frac{1}{\nu} V_x \quad (13)$$

Integrating both sides of Equation (13), we get

$$\phi = \frac{1}{2\nu} V_x^2 + C_1 \quad (14)$$

In Equation (14),  $C_1$  is the integration constant, which can be evaluated by applying boundary conditions. We can set the boundary condition as:

$$\text{At } V_x = 0, \phi = \frac{dV_x}{dx} = 0$$

Applying this boundary condition to Equation (14), we have

$$\phi = \frac{1}{2\nu} V_x^2 \quad (15)$$

Equating Equation (15), and applying the boundary condition, we have the value for  $x$  as:

$$x = -\nu + \sqrt{\nu^2 + 4\nu t} \quad (16)$$

Further calculation yields the x-component velocity,  $v_x$ , as:

$$v_x = \frac{1}{\sqrt{\nu t}} \quad (17)$$

2) *Y-component Equation:* Rearranging Equation (9), we can write it as:

$$\frac{d^2 V_y}{dy^2} - \frac{1}{\nu} \frac{dV_y}{dt} = 0 \quad (18)$$

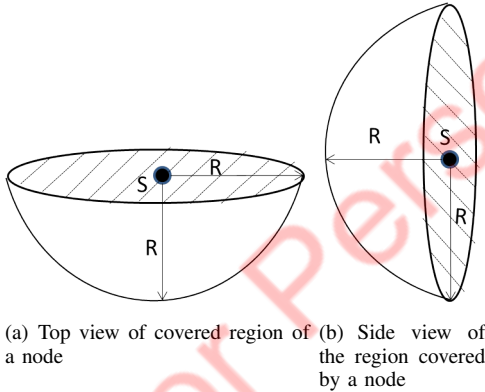


Fig. 1: Projection of a plane of the region covered by a sensor node in 3-D space

Let,  $\psi(V_y) = \frac{dV_y}{dy}$ . So,  $\frac{d^2 V_y}{dy^2} = \frac{d}{dy}(\psi) = \psi \frac{d\psi}{dV_y}$ . Substituting these values in Equation (18), we have the finalized expression for Y-component as:

$$\psi \frac{d\psi}{dV_y} - \frac{1}{\nu} \psi V_y = 0 \quad (19)$$

Equation (19) is similar to Equation (12). Therefore, proceeding in the same way as we did for X-component, and applying the same boundary conditions, we get the expression for  $y$  as:

$$y = -\nu + \sqrt{\nu^2 + 4\nu t} \quad (20)$$

Similarly, we get the y-component velocity,  $v_y$ , of a node at any instant  $t$  as:

$$v_y = \frac{1}{\sqrt{\nu t}} \quad (21)$$

3) *Z-component Equation:* Rearranging Equation (10), we can write it as:

$$\frac{d^2 V_z}{dz^2} - \frac{1}{\nu} V_z \frac{dV_z}{dZ} - \frac{1}{\nu \rho} \frac{\partial p}{\partial z} - \frac{1}{\nu} g = 0 \quad (22)$$

In Equation (22),  $p$  is the dynamic pressure. In terms of  $V_z$ , the dynamic pressure is expressed as:

$$p = \frac{1}{2} \rho V_z^2 \quad (23)$$

Carrying out partial derivative of dynamic pressure with respect to  $z$ , we get

$$\frac{1}{\rho} \frac{\partial p}{\partial z} = V_z \frac{\partial V_z}{\partial z} \quad (24)$$

Substituting this value from Equation (24) to the Equation (22), we have

$$\frac{d^2 V_z}{dV_z^2} - \frac{2}{\nu} V_z \frac{dV_z}{dZ} - \frac{1}{\nu} g = 0 \quad (25)$$

We can write the Equation (25) as:

$$\frac{d}{dz} \left[ \frac{dV_z}{dz} - \frac{1}{\nu} V_z^2 \right] = \frac{1}{\nu} g \quad (26)$$

Integrating both sides of Equation (26), we get

$$\frac{dV_z}{dz} - \frac{1}{\nu} [V_z^2 + gZ] = C_3 \quad (27)$$

In Equation (27),  $C_3$  is the integration constant, which can be evaluated by applying the boundary condition as:

$$\text{At } z = 0, V_z = 0, \text{ and } \frac{dV_z}{dz} = 0.$$

By applying the boundary condition above, we get the value of integration constant,  $C_3 = 0$ . Therefore, Equation (27) can be rewritten as:

$$\frac{dV_z}{dz} - \frac{1}{\nu} [V_z^2 + gZ] = 0 \quad (28a)$$

$$\frac{dV_z}{dz} = \frac{1}{\nu} [V_z^2 + gZ] \quad (28b)$$

Equation (28a) is the special form of Riccati equation, which is non-linear in  $V_z$ . We did not get any closed form solution of Equation (28a). Therefore, we had to resort to numerical techniques to solve the equation. We solved it using Euler's numerical method. The steps we have followed to set up the numerical equations are given below.

**Step 1:** We write the equation in the form as:

$$\frac{dV_z}{dz} = f(z, V_z) \quad (29)$$

In Equation (29), the function  $f$  can be written in this context as:

$$f(z, V_z) = \frac{1}{\nu} [V_z^2 + gz] \quad (30)$$

**Step 2:** Let us take the step size as  $\delta z$ , and the maximum number of steps to be a positive number  $N$ . A maximum value

of  $z$  is taken as  $z_{max}$ . The parameters have been chosen in such a way that,

$$z_{max} = z_0 + N\Delta z \quad (31)$$

In Equation (31),  $z_0$  is the initial value of  $z$ , which has been set as zero. According to the Euler's numerical technique, the smaller the step size, the better the accuracy. We have taken the step size  $\Delta z = \frac{1}{2} = 0.5$ , and the maximum steps  $N = 6$ . Therefore,

$$z_{max} = z_0 + 6 \cdot \frac{1}{2} = 3 \quad (32)$$

**Step 3:** Let us write the parametric equations as:

$$z_{n+1} = z_n + \Delta z \quad (33)$$

$$(V_z)_{n+1} = (V_z)_n + \Delta z \cdot f[z_n, (V_z)_n] \quad (34)$$

In Equation (33), the function,  $f$ , can be expressed as:

$$f[z_n, (V_z)_n] = \frac{1}{\nu} [(V_z)_n^2 + gz_n] \quad (35)$$

Taking the value of  $f$ , the parameters can be expressed as:

$$z_{n+1} = z_n + \frac{1}{2} \quad (36)$$

$$(V_z)_{n+1} = (V_z)_n + \frac{1}{2\nu} [(V_z)_n^2 + gz_n] \quad (37)$$

Next, step-wise *iterative computations* are carried out, as shown below.

**Step 1:** Compute the values of  $z_1$  and  $(V_z)_1$  with  $n = 0$ . According to the Equations (36) and (37), we can write:

$$z_1 = z_{0+1} = 0 + \frac{1}{2} = 0.5 \quad (38)$$

$$(V_z)_1 = (V_z)_{0+1} = (V_z)_0 + \frac{1}{2\nu} [(V_z)_0^2 + gz_0] = 0 \quad (39)$$

**Step 2:** Calculate  $z_2$  and  $(V_z)_2$  by setting  $n = 1$ .

$$z_2 = z_{1+1} = z_1 + \Delta z = \frac{1}{2} + \frac{1}{2} = 1 \quad (40)$$

$$(V_z)_2 = (V_z)_1 + \frac{1}{2\nu} [0 + g \cdot \frac{1}{2}] = \frac{g}{4\nu} \quad (41)$$

**Step 3:** Calculate  $z_3$  and  $(V_z)_3$  by setting  $n = 2$ .

$$z_3 = \frac{3}{2} \quad (42)$$

$$(V_z)_3 = \frac{g}{4\nu} + \frac{1}{2\nu} \left[ \left( \frac{g}{4\nu} \right)^2 + g \right] \quad (43)$$

**Step 4:** Calculate  $z_4$  and  $(V_z)_4$  by setting  $n = 3$ .

$$z_4 = 2 \quad (44)$$

$$(V_z)_4 = (V_z)_3 + \frac{1}{2\nu} \left[ \left( (V_z)_3 \right)^2 + \frac{3}{2}g \right] \quad (45)$$

**Step 5:** Calculate  $z_5$  and  $(V_z)_5$  by setting  $n = 4$ .

$$z_5 = \frac{5}{2} \quad (46)$$

$$(V_z)_5 = (V_z)_4 + \frac{1}{2\nu} \left[ \left( (V_z)_4 \right)^2 + 2g \right] \quad (47)$$

**Step 6:** Calculate  $z_6$  and  $(V_z)_6$  by setting  $n = 5$ .

$$z_6 = 3 \quad (48)$$

$$(V_z)_6 = (V_z)_5 + \frac{1}{2\nu} \left[ \left( (V_z)_5 \right)^2 + \frac{5}{2}g \right] \quad (49)$$

The numerical values of the computations are shown in Table I.

We observe from Table I that the average value of the  $Z$ -component of velocity of a sensor node is 2.35. However, in reality, a node cannot move with constant velocity in the vertical plane of an ocean. Near to the surface, a node moves faster than when we go deeper into it. We have assumed that a node has exponential decay in velocity with increasing depth in a vertical plane of ocean. On the basis of this assumption, we have expressed the vertical component of a node's velocity,  $V_z$  as:

$$V_z = 2.35 \times \exp(-gvz) \quad (50)$$

In Equation (50),  $g$  is the gravitational acceleration having value  $9.8 \text{ m/s}^2$ . We express  $V_z$  as  $\frac{dz}{dt}$ . Through mathematical computations and applying the boundary condition (at  $t = 0$ ,  $z = 0$ ) to the Equation (50), we can express the position of a node at any instant  $t$  in the vertical plane as:

$$z = \frac{1}{gv} \log(2.35 \times vt + 1) \quad (51)$$

## V. NETWORK CHARACTERIZATION

Any mobile network can be represented in terms of time varying graph as [28]:

$$\Phi = \{N(t), e(t)\} \quad (52)$$

In Equation (52),  $N(t)$  denotes a set of nodes moving in a plane at any instant  $t$ , and  $e(t)$  denotes the communication link established between any two nodes,  $(n_i, n_j) \in e(t)$ , while they are in the communication range of each other. In this scenario,  $e(t)$  is the acoustic link between any two nodes, where one node acts as the sender of packet and another as receiver. The formation of link between two nodes is shown in Figure 3.

The concern is with  $e(t)$ , as this parameter randomly varies over time due to the dynamic nature of channel. However, even if the nodes are in the communication range of each other, link disruption might take place due to signal's interference with ocean ambient noise, signal diffraction, shadowing and reflection.

## VI. EFFECT OF NODE MOBILITY ON UWASNS

Due to the mobility of the channel, some physical parameters relevant to sensor networks change over space and time. In

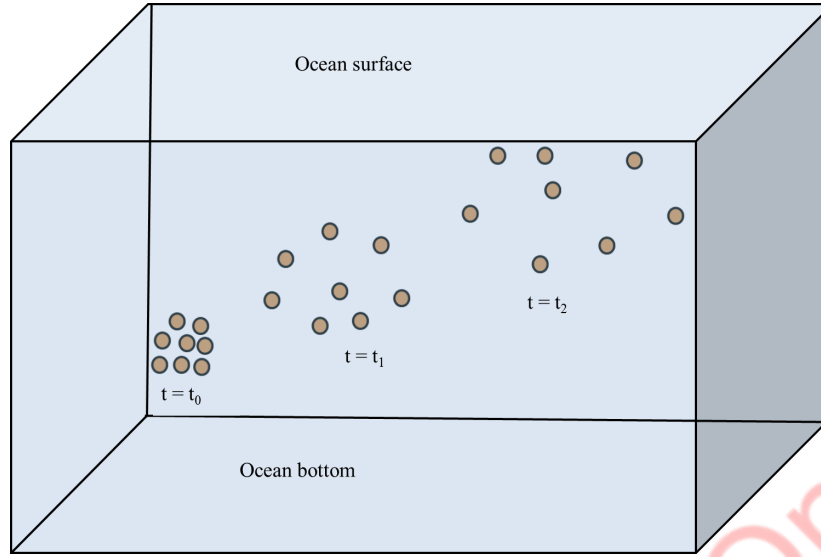


Fig. 2: Node dispersion in the 3-D ocean column

<b>n</b>	$z_n$	$(V_z)_n$	$\alpha$	<b>Final</b> $(V_z)_n$
1	$\frac{1}{2}$	0	0	0
2	1	$2.333 \times 10^6$	$10^{-6}$	2.333
3	$\frac{3}{2}$	$2.593 \times 10^{18}$	$10^{-18}$	2.593
4	2	$3.201 \times 10^{42}$	$10^{-42}$	3.201
5	$\frac{5}{2}$	$4.878 \times 10^{90}$	$10^{-90}$	4.878
6	3	$1.133 \times 10^{187}$	$10^{-187}$	1.133

TABLE I: Results of Euler's method to solve  $V'_z = \frac{1}{\nu}[V_z^2 + gZ]$  with  $V_z(0) = 0$ , using step size  $\delta z = \frac{1}{2}$ , maximum no of steps  $n = 6$ .

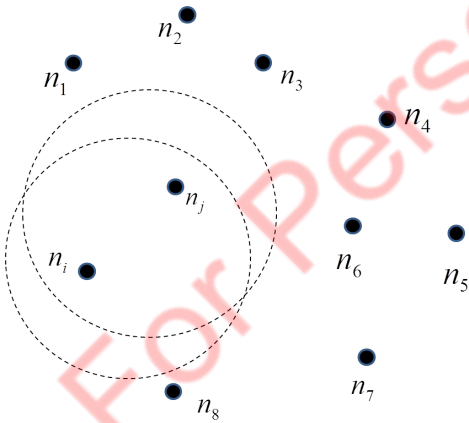


Fig. 3: Formation of graph for each pair of nodes

this Section, we present the parameters which are considered in this work.

#### A. Dispersion

Due to channel mobility, sensor nodes disperse from their initial positions. This dispersion takes place in 3-D. The

average dispersion per node in the 3-D space is given as [36]:

$$\Delta(r, t) = \frac{1}{N} \sum_{i=1}^N |r_i(t) - r_i(t_0)|^2 \quad (53)$$

Where  $N$  is the total number of nodes deployed,  $r_i(t)$  and  $r_i(t_0)$  are, respectively, the position vectors at any time  $t$  and at initial time  $t_0$  of  $i^{th}$  node. Square sign on the right hand side of Equation (53) signifies that irrespective of the sign of position vectors, dispersion is always positive valued. The physical scenario of node's dispersion is shown in Figure 2.

#### B. Coverage and Connectivity

Any node can cover the region belonging to its transmission range in all directions. We have considered all the nodes to be homogeneous in nature in terms of sensing capability. Therefore, each and every node has equal transmission range. Here, we have assumed that a node can cover a spherical region of radius  $R$  centered at that node's position. We have depicted the scenario in Figure 1.

A communication link is established between any two nodes when they are in the communication range of each other. Due to the adverse and hostile oceanic underwater channel, a node suffers from hardware vulnerability and resource limitations. Nodes are resource limited because unlike terrestrial WSNs,

where in most cases the nodes can be recharged due to favourable deployable channel, in underwater environment, nodes of the network cannot be recharged. Keeping in mind the above mentioned aspects, we infer that over time a node's coverage region decreases with respect to the maximum area it can cover. The physical scenario is shown in Figure 4.

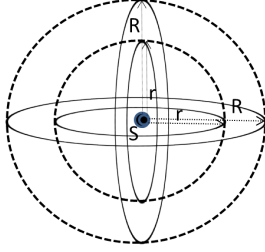


Fig. 4: Fraction of region covered by a node

We express the fractional area covered by a node as:

$$f_A = \frac{\frac{4}{3}\pi r^3}{\frac{4}{3}\pi R^3} = \left(\frac{r}{R}\right)^3 \quad (54)$$

In the Equation (54),  $r$  is the range of a node at any time  $t$ .

### C. Localization

Node localization refers to finding the location of the deployed nodes. The knowledge of node location facilitates the extraction of meaningful insights from the sensed information. Also, the successful execution of the geographic routing schemes depend on the knowledge of location information. However, in UWASNs, we require specific node localization schemes, which address the challenges of this type of networks. Moreover, unlike the terrestrial wireless sensor networks, Global Positioning System (GPS) can not be applied to UWASNs due to the severe attenuation of RF signal. In recent times, different localization schemes are proposed for UWASNs. Tan et al. [37] and Erol-Kantarci et al. [38] presented a survey of these schemes. The existing schemes are classified into various categories — *anchor-based* or *anchor-free*, *range-based* or *range-free*, and *centralized* or *distributed*. These different schemes looked into designing energy-efficient, scalable, highly convergent, and node mobility- and sparsity-adaptive node localization.

In Figure 5, we demonstrate a typical node localization scenario. In this figure,  $s$  is the unlocalized node, and  $A_1$ ,  $A_2$ , and  $A_3$  are the anchor nodes, which have the knowledge of their own locations. Node  $s$  receives ‘location beacons’ from the anchors, and measures the time-of-arrival ( $t_{i,s}$ ,  $\forall i \in \{A_1, A_2, A_3\}$ ) of each beacon. Next, node  $s$  computes the inter-node distance with the anchors,  $d_{i,s} = t_{i,s} \times V_{acoustic}$ . Based on these information, the location of the unlocalized sensor nodes can be computed by solving Equations (55), (56), and (57).

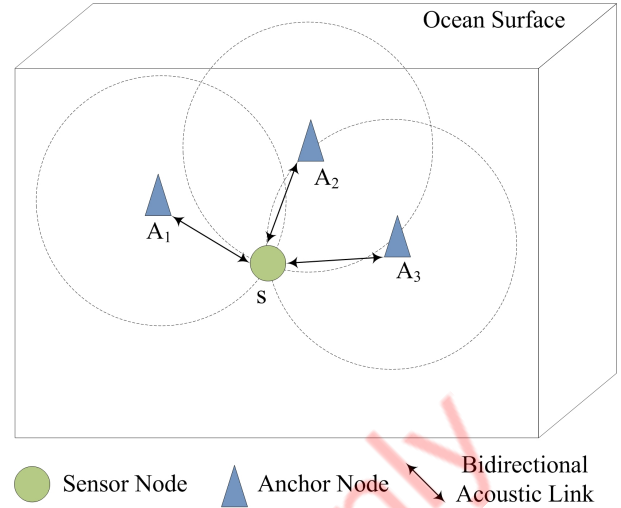


Fig. 5: Localization by anchored nodes

$$(x - x_1)^2 + (y - y_1)^2 + (z - z_1)^2 = d_{A_1,s}^2 \quad (55)$$

$$(x - x_2)^2 + (y - y_2)^2 + (z - z_2)^2 = d_{A_2,s}^2 \quad (56)$$

$$(x - x_3)^2 + (y - y_3)^2 + (z - z_3)^2 = d_{A_3,s}^2 \quad (57)$$

where  $(x_i, y_i, z_i)$  denotes the location of any anchor  $i \in \{A_1, A_2, A_3\}$ .

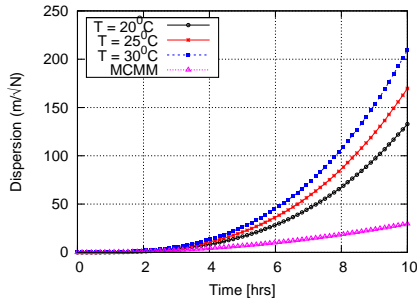
TABLE II: Simulation Parameters

Parameters	Values
Deployment Region	2000 m × 2000 m × 2000 m
Number of nodes (N)	50, 75, 100
Transmission range	1500 m
Transmission power	0.203 watts
Receive power	0.024 watts
Initial energy of a node	200 Joule
Threshold battery level	50 Joule
Temperature (T)	20 <sup>0</sup> C, 25 <sup>0</sup> C, 30 <sup>0</sup> C
Kinematic viscosity ( $\nu$ )	(1.16, 1.17, 1.18) × 10 <sup>-6</sup> m <sup>2</sup> /s
Spreading co-efficient	1.5
Noise model	ambient noise model

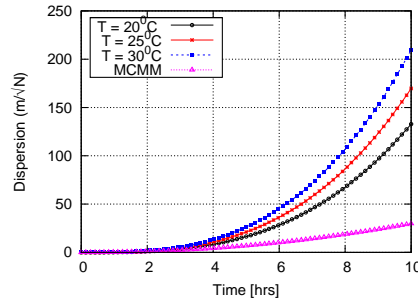
## VII. PERFORMANCE EVALUATION

### A. Simulation Settings

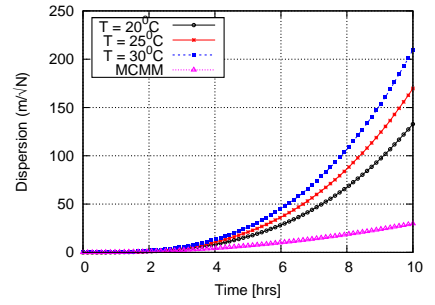
We have used NS-3 (<http://www.nsnam.org/>) simulator for the performance evaluation of our work. The simulation region was set at 2000 m × 2000 m × 2000 m. In different experiments, we consider UWASNs with 50, 75, 100 nodes randomly deployed in the simulation region. Initially, the nodes were densely deployed. However, with time, the nodes diverge, due to which, the node density fluctuates with time. It is noteworthy to mention that the movement of nodes was not restricted by the simulation region boundary. Rather, the initial placement of the nodes was inside the simulation boundary. We adopted the *Ambient noise model* [39] and *Thorpe model* [40] for simulating the underwater channel and



(a) Dispersion for N = 50

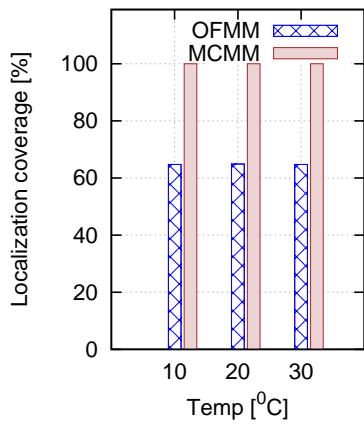


(b) Dispersion for N = 75

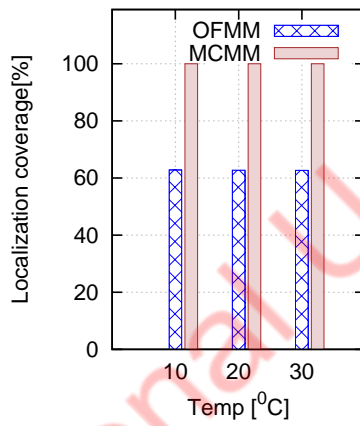


(c) Dispersion for N = 100

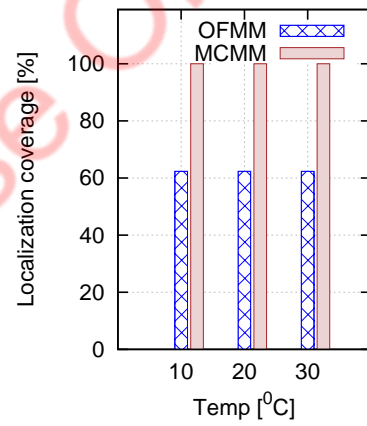
Fig. 6: Dispersion of nodes



(a) Dispersion for N = 50

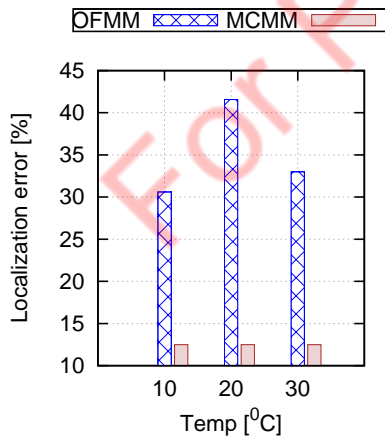


(b) Dispersion for N = 75

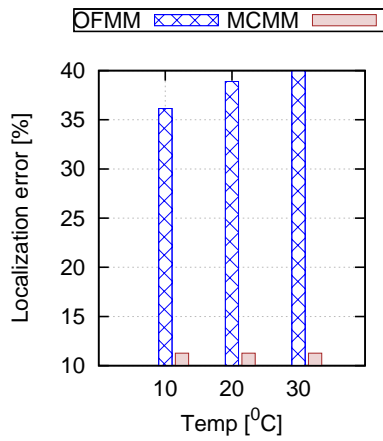


(c) Dispersion for N = 100

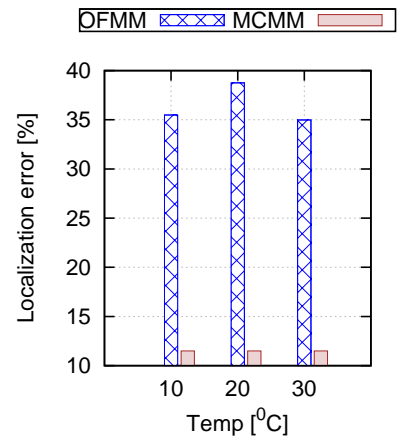
Fig. 7: Localization coverage of nodes



(a) Dispersion for N = 50



(b) Dispersion for N = 75



(c) Dispersion for N = 100

Fig. 8: Localization error of nodes

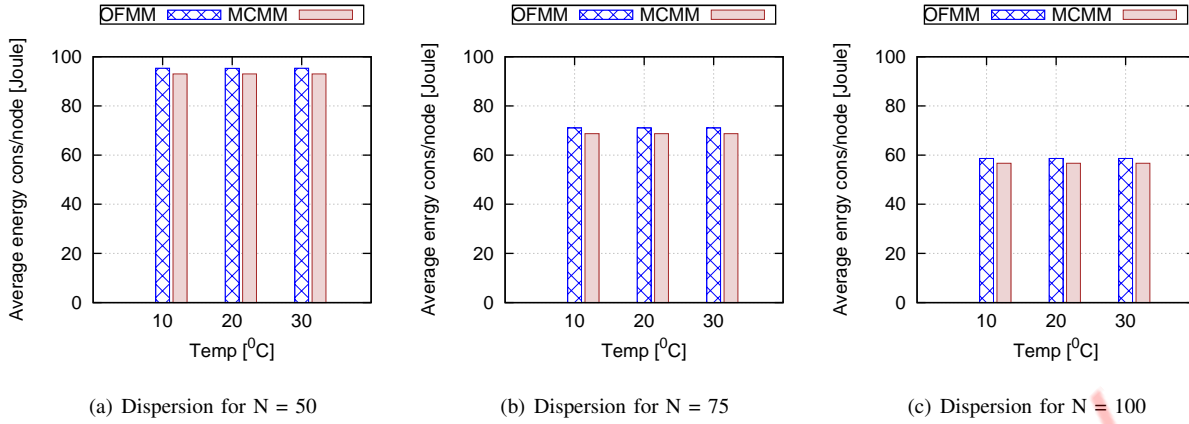


Fig. 9: Average energy consumption per node

signal propagation. The simulation of the proposed model was executed with different water temperatures ( $T$ ) set at 20 °C, 25 °C, and 30 °C. The rest of the simulation parameters are listed in Table II.

### B. Benchmark

To the best of our knowledge, there exists no mobility model representing 3-D movement of nodes in underwater ocean. The existing models (e.g. [28], [31], [32]) only describe the movement of networking nodes in 2-D horizontal plane. Among these, the Meandering Current Mobility Model (MCMM) [28] is a standard one representing the 2-D movement of sensor nodes under the influence of subsurface jet current. In MCMM, the authors show that the nodes disperse with time due to the effects of the sub-surface jet currents. Along with dispersion, the authors also considered others metrics too. Therefore, we compare the performance of the proposed mobility model (OFMM) with the existing Meandering Current Mobility Model (MCMM).

### C. Results and Discussions

In this section, we discuss the metrics representing the performance of the mobile UWASNs.

1) *Dispersion*: In Figure 6, we show node's dispersion at different temperatures for OFMM and compared the results with MCMM. From Figure 6, we observe that the dispersion of nodes in the proposed mobility model with time is more than that of the MCMM model. Additionally, we observe that with the increase in temperature, dispersion also increases. Dispersion mainly depends on the associated forces experienced by the nodes in the oceanic medium. In MCMM, the nodes are assumed to be dispersed under the influence of 2-D subsurface jet current. However, in OFMM, we consider the nodes to be persuaded by more number of oceanic forces, and they disperse in the 3-D channel. With the increase in temperature, the effect of force on node's mobility modulates and node's mobility also has direct dependency on the kinematic viscosity,  $\nu$ . Calculation shows that, compared to MCMM, dispersion in the proposed model, OFMM, increases by 21.5%.

2) *Localization coverage*: Figure 7 shows localization coverage of the nodes. As node dispersion in OFMM is more than that of the MCMM, node density changes rapidly. As a consequence of which the localization coverage decreases. From Figure 7, we observe that localization coverage for MCMM is more than that of OFMM. Simulation results show that localization coverage for our model decreases by 36.70%.

3) *Localization error*: Figure 8 shows the localization error of nodes. We observe that the localization error in our model is more that of MCMM. As node density rapidly changes with time, the estimation of the location of a node in the proposed model, OFMM, is more than that in MCMM. It is observed that localization error increases by 21.14%.

4) *Average energy consumption per node*: Figure 9 shows the energy consumed per node in the network. It is evident that the energy consumed per node using the proposed model is more than using MCMM. Due to the increased dispersion of nodes with time, more number of underwater beacons are required to localize a node. For broadcasting more number of beacon messages, more amount of energy is required for a node. Calculation shows that in our model, the average energy consumption per node increases by 3%.

## VIII. CONCLUSION

In this paper, we present a node mobility model, named Oceanic Forces Mobility Model (OFMM), for UWASNs by considering the major oceanic forces. We discuss the major oceanic forces instrumental in passive mobility of deployed nodes. Thereafter, we analyze the performance of UWASNs in terms of network dispersion and node localization. Simulation based results are presented to validate the proposed model. Results indicate that the network dispersion increases by 21.5% compared to the existing Meandering Current Mobility Model (MCMM). In terms of node localization, in OFMM, we observed a decrease in localization coverage by nearly 36.70%, an increase in localization error by nearly 21.14%, and an increase in average energy consumption per node by nearly 3%, compared to the MCMM model.

In the present work, we considered the underwater nodes to be moving under the influence of oceanic forces only. However, we excluded the consideration of mutual interaction of nodes. In the future, we want to evaluate the performance of UWASNs in a scenario where the underwater nodes move due to the combined effect of oceanic forces and mutual interaction with each other. Also, the model's performance may be evaluated in shallow oceanic regions, and in polar water containing large number of icebergs.

## REFERENCES

- [1] T. Melodia, H. Kulhandjian, L.-C. Kuo, and E. Demirors, *Advances in Underwater Acoustic Networking*, ser. Mobile Ad Hoc Networking: Cutting Edge Directions, Second Edition. Wiley Online Library, 2013.
- [2] J. Heidemann, M. Stojanovic, and M. Zorzi, "Underwater sensor networks: Applications, advances and challenges," *Philosophical Transaction of the Royal Society A*, vol. 370, no. 1958, pp. 158–175, 2012.
- [3] I. F. Akyildiz, D. Pompili, and T. Melodia, "Underwater acoustic sensor networks: research challenges," *Ad-Hoc Networks*, vol. 3, no. 3, pp. 257–279, 2005.
- [4] M. S. Obaidat and S. Misra, *Principles of Wireless Sensor Networks*. Cambridge University Press, U.K., 2014.
- [5] B. M. Howe, Y. Chao, P. Arabshahi, S. Roy, T. McGinnis, and A. Gray, "A smart sensor web for ocean observation: Fixed and mobile platforms, integrated acoustics, satellites and predictive modeling," *IEEE Journal of Selected Topics in Applied Earth Observations and Remote Sensing*, vol. 3, no. 4, pp. 507–521, 2010.
- [6] K. Christidis, P. Nikipolitis, G. I. Papadimitriou, P. G. Sarigiannidis, and A. S. Pomportsis, "Utilizing locality of demand for lower response times in underwater data broadcasting," in *Proceedings of IEEE Vehicular Technology Conference (VTC Spring)*, Budapest, Hungary, 2011, pp. 1–5.
- [7] S. Misra, S. Singh, M. Khatua, and M. S. Obaidat, "Extracting mobility pattern from target trajectory in wireless sensor networks," *International Journal of Communication Systems*, 2013 [DOI: 10.1002/dac.2649].
- [8] G. Isbitiren and O. B. Akan, "Three-dimensional underwater target tracking with acoustic sensor networks," *IEEE Transactions on Vehicular Technology*, vol. 60, no. 8, pp. 3897–3906, 2011.
- [9] A. K. Mandal, S. Misra, M. K. Dash, and T. Ojha, "Performance analysis of distributed underwater wireless acoustic sensor networks in the presence of internal solitons," *International Journal of Communication Systems*, 2014 [DOI: 10.1002/dac.2843].
- [10] J. Partan, J. Kurose, B. N. Levine, "A survey of practical issues in underwater networks," in *Proceedings of ACM WUWNet*, Los Angeles, CA, USA, 2006, pp. 17–24.
- [11] E. M. Sozer, M. Stojanovic, J. G. Proakis, "Underwater acoustic networks," *IEEE Journal of Oceanic Engineering*, vol. 25, no. 1, pp. 72–83, 2000.
- [12] S. K. Dhurandher, S. Misra, M. S. Obaidat and S. Khairwal, "UWSim: An underwater sensor network simulator," *Transactions of the Society for Modeling and Simulation International*, vol. 84, no. 7, pp. 327–338, 2008.
- [13] M. K. Watfa, S. Selman, and H. Denkilian, "UW-MAC: An underwater sensor network MAC protocol," *International Journal of Communication Systems*, vol. 23, no. 4, pp. 485–506, 2010.
- [14] S. K. Dhurandher, M. S. Obaidat, and M. Gupta, "Providing reliable and link stability-based geocasting model in underwater environment," *International Journal of Communication Systems*, 2012 [DOI: 10.1002/dac.1245].
- [15] F. Bai, K. S. Munasinghe, and A. Jamalipour, "Accuracy, latency, and energy cross-optimization in wireless sensor networks through infection spreading," *International Journal of Communication Systems*, vol. 24, no. 5, pp. 628–646, 2011.
- [16] J. H. Cui, J. Kong, M. Gerla, S. Zhou, "The challenges of building scalable mobile underwater wireless sensor networks for aquatic applications," *IEEE Network*, vol. 20, no. 3, pp. 12–18, 2006.
- [17] T. Ojha, M. Khatua, and S. Misra, "Tic-Tac-Toe-Arch: A self-organizing virtual architecture for underwater sensor networks," *IET Wireless Sensor Systems*, vol. 3, no. 4, pp. 307–316, 2013.
- [18] S. Misra, T. Ojha, A. Mondal, "Game-theoretic topology control for opportunistic localization in sparse underwater sensor networks," *IEEE Transactions on Mobile Computing*, vol. 13, 2014 [DOI: 10.1109/TMC.2014.2338293].
- [19] M. T. Isik and O. B. Akan, "A three dimensional localization algorithm for underwater acoustic sensor networks," *IEEE Transactions on Wireless Communications*, vol. 8, no. 9, pp. 4457–4463, 2009.
- [20] S. Misra, S. Dash, M. Khatua, A. Vasilakos and M. S. Obaidat, "Jamming in underwater sensor networks: Detection and mitigation," *IET Communications*, vol. 6, no. 14, pp. 2178–2188, 2012.
- [21] M. Khatua and S. Misra, "Exploiting partial-packet information for reactive jamming detection: studies in uwsn environment," in *Proceedings of the 14<sup>th</sup> International Conference on Distributed Computing and Networking (ICDCN 2013)*, ser. Springer Lecture Notes in Computer Science (LNCS), vol. 7730, Mumbai, 2013, pp. 118–132.
- [22] A. Wahid, S. Lee, D. Kim, "A reliable and energy-efficient routing protocol for underwater wireless sensor networks," *International Journal of Communication Systems*, 2012 [DOI: 10.1002/dac.2455].
- [23] L. W. Chang, Y. M. Huang, C. C. Lin, "Performance analysis of S-MAC protocol," *International Journal of Communication Systems*, vol. 26, pp. 1129–1142, 2013.
- [24] A. V. Babu and S. Joshy, "Maximizing the data transmission rate of a cooperative relay system in an underwater acoustic channel," *International Journal of Communication Systems*, vol. 25, pp. 231–253, 2012.
- [25] J. Partan, J. Kurose, B. N. Levine, "A survey of practical issues in underwater networks," *ACM SIGMOBILE Mobile Computing and Communications Review*, vol. 11, no. 4, pp. 23–33, 2006.
- [26] D. Pompili, T. Melodia, I. F. Akyildiz, "Three-dimensional and two-dimensional deployment analysis for underwater acoustic sensor networks," *Ad-Hoc Networks*, vol. 7, no. 4, pp. 778–790, 2009.
- [27] J. Liu, Z. Zhou, Z. Peng, J-H Cui, M. Zuba, L. Fiondella, "Mobi-sync: efficient time synchronization for mobile underwater sensor networks," *IEEE Transaction on Parallel and Distributed Systems*, vol. 24, no. 2, pp. 406–416, 2013.
- [28] A. Caruso, F. Paparella, L. F. M. Vieira, M. Erol, M. Grella, "The meandering current mobility model and its impact on underwater mobile sensor networks," in *Proceedings of IEEE INFOCOM*, Phoenix, AZ, 2008, pp. 771–779.
- [29] M. Erol, S. Oktug, "A localization and routing framework for mobile underwater sensor networks," in *Proceedings of IEEE INFOCOM Workshops*, Phoenix, AZ, 2008, pp. 1–3.
- [30] J. Luo, D. Wang, Q. Zhang, "Double mobility: coverage of the sea surface with mobile sensor networks," in *Proceedings of IEEE INFOCOM*, Rio de Janeiro, Brazil, 2009, pp. 118–126.
- [31] M. Erol-Kantarci, S. Oktug, L. Vieira, M. Gerla, "Performance evaluation of distributed localization techniques for mobile underwater acoustic sensor networks," *Ad-Hoc Networks*, vol. 9, no. 1, pp. 61–72, 2010.
- [32] Z. Yang, S. Cai, N. Yao, H. Pan, Q. Han, *The node movement models based on lagrange motion for 3-D underwater acoustic sensor network*. Berlin Heidelberg: Springer-Verlag, 2012, pp. 685–693.
- [33] A. Kostin, G. Oz, H. Haci, "Performance study of a wireless mobile ad-hoc network with orientation dependent internode communication scheme," *International Journal of Communication Systems*, vol. 27, no. 2, pp. 322–340, 2014.
- [34] S. Pond, G. L. Pickard, *Introductory dynamical oceanography*, 2nd ed. Butterworth-Heinemann, 1978.
- [35] R. H. Stewart, *Introduction to physical oceanography*. Department of Oceanography, Texas A & M University: Texas A & M University, 2004.
- [36] A. Provenzale, "Transport by coherent barotropic vortices," *Annual Review of Fluid Mechanics*, vol. 31, no. 1, pp. 55–93, 1999.
- [37] H.-P. Tan, R. Diamant, W. K. G. Seah, and M. Waldmeyer, "A survey of techniques and challenges in underwater localization," *Ocean Engineering*, vol. 38, no. 14, pp. 1663–1676, 2011.
- [38] M. Erol-Kantarci, H. T. Mouftah, and S. Oktug, "A survey of architectures and localization techniques for underwater acoustic sensor networks," *IEEE Communications Surveys and Tutorials*, vol. 13, no. 3, pp. 487–502, 2011.
- [39] A. F. Harris, M. Zorzi, "Modeling the underwater acoustic channel in NS2," in *Proceedings of the 2<sup>nd</sup> International Conference on Performance Evaluation Methodologies and Tools*, Nantes, France, 2007, p. 18.
- [40] W. H. Thorp, "Analytic description of the low frequency attenuation coefficient," *Journal of Acoustical Society of America*, vol. 42, no. 1, p. 270, 1967.